Supercritical bifurcation of a spinning hoop

Frédéric Moisy[a)]
FAST, Bât. 502, Campus Universitaire, 91405 Orsay Cedex, France

(Received 18 November 2002; accepted 18 April 2003)

The motion of a hoop hung on a spinning string provides an illustrative and pedagogical example of a supercritical bifurcation. Above a certain angular velocity threshold Ω_c, the hoop rises and spins about its symmetry axis. The equation of motion is derived in the limit of a long massless string, and the calculated steady states are compared to experimental measurements. This simple experiment is suitable for classroom demonstration, and provides an interesting alternative to the classical experiment of a bead sliding on a rotating hoop. © *2003 American Association of Physics Teachers.*
[DOI: 10.1119/1.1582191]

I. INTRODUCTION

The rotation of rigid bodies often displays interesting instability problems. Bodies with three different moments of inertia are well known to have unstable rotation about the intermediate axis,[1] as commonly observed from acrobatic jumps or dives. Throwing a tennis racket provides an easy illustration of this instability of free rotation. Such purely inertial instability has no threshold, i.e., it can be observed for very low rotation rates. In contrast, for axisymmetric bodies such as hoops, disks, rockets, eggs, etc., the free rotations remain stable, but different mechanisms may also lead to instability when external forces are present. Under some circumstances, spectacular and unexpected instabilities may originate from frictional forces. This is the case for the tippe-top, a popular toy that flips over and rotates on its stem, or for the hard-boiled egg problem, which has recently received a nice analysis.[2] The competition between gravity and centrifugal forces may lead to an instability with a finite rotation rate threshold,[3] as illustrated by the simple experiment described in this paper.

A hoop is hung on a long string, whose upper end is spun. At low rotation rate, the hoop is vertical and simply spins about its diameter. As the rotation rate is increased, the hoop progressively rises and becomes horizontal, spinning about its symmetry axis, while the string moves along a cone. This situation may appear paradoxical, since the horizontal position maximizes both kinetic and potential energy. The popular ''hula hoop'' game, where the string rotation is replaced by the oscillations of the player's hips, is a common illustration of this phenomenon. It is similar to the conical pendulum problem,[1] usually illustrated in the classical demonstration experiment of the bead sliding along a vertically rotating hoop.[4–7]

In this paper, the equation of motion is derived from Lagrange's equation. An alternate derivation, from the angular momentum equation, is also presented as a good illustration of the dynamics of a rigid body. The hoop is shown to rise following a supercritical bifurcation for the string rotation rate Ω above a critical value $\Omega_c=(2g/R)^{1/2}$, where g is the gravitational acceleration and R is the hoop radius. The stable solution, $\theta_{\rm eq}=\cos^{-1}(\Omega_c/\Omega)^2\propto(\Omega-\Omega_c)^{1/2}$ for $\Omega-\Omega_c \ll 1$, coincides with that of the conical pendulum or the bead-on-a-hoop. The nonlinear oscillations are briefly described by means of phase portraits, and compared to that of the bead-on-a-hoop. Simple considerations from string torsion and air friction allow us to estimate the startup and damping timescales. Finally some experimental measurements are reported, and are shown to compare well with the theoretical solution.

In this experiment the angular rotation threshold is of the order of a few rad/s, and thus the string can be simply spun with the fingers. Because it only requires a string and a hoop, this experiment can be conveniently used as a classroom illustration of spontaneous symmetry breaking and bifurcation. Although the detail of the calculation is somewhat more subtle than that of the classical bead-on-a-hoop problem, because it deals with rigid body dynamics, the physics is basically the same and does not require the much heavier apparatus of the bead-on-a-hoop demonstration.

II. THEORY

A. Equation of motion

We consider a thin uniform hoop, of radius R and mass m, fixed at a point P on its periphery by a massless string of length $L \gg R$ (see Fig. 1). The string is spun from its other end O at a constant angular velocity Ω. The center of mass G is assumed to remain vertically aligned with the point O.

In addition to the natural coordinates $(\mathbf{e}_x,\mathbf{e}_y,\mathbf{e}_z)$, where $\mathbf{e}_z$ is vertically upwards, we introduce the rotating frame $(\mathbf{e}_1,\mathbf{e}_2,\mathbf{e}_3)$ attached to the hoop. We label $\mathbf{e}_3$ the symmetry axis of the hoop, and $\mathbf{e}_1$ the axis from the center of the hoop to the point P where the string is tied up, which makes an angle θ with the vertical axis. We consider for simplicity a zero roll angle about $\mathbf{e}_1$, i.e., we assume that the point P is the highest point of the hoop, so that the axis $\mathbf{e}_2$ remains horizontal.

Let us first consider a rigid string, so that the hoop angular velocity $\dot{\phi}$ about the vertical axis $\mathbf{e}_z$ instantaneously follows the imposed angular velocity Ω. The pitch angle θ is then the only degree of freedom for this problem. The total angular velocity $\boldsymbol{\omega}$ of the hoop has two contributions. The first one, of magnitude Ω, is imposed from O through the string, and is about $\mathbf{e}_z=\cos\theta\,\mathbf{e}_1+\sin\theta\,\mathbf{e}_3$ (the points O and G are at rest, so that OG is the instantaneous axis of rotation when θ is kept constant). The second one comes from the pitch variation $\dot{\theta}$, and is about the axis $\mathbf{e}_2$. Hence, the total angular velocity in the frame $(\mathbf{e}_1,\mathbf{e}_2,\mathbf{e}_3)$ can be written

$$\boldsymbol{\omega}=\begin{pmatrix}\Omega\cos\theta\\ \dot{\theta}\\ \Omega\sin\theta\end{pmatrix}. \tag{1}$$

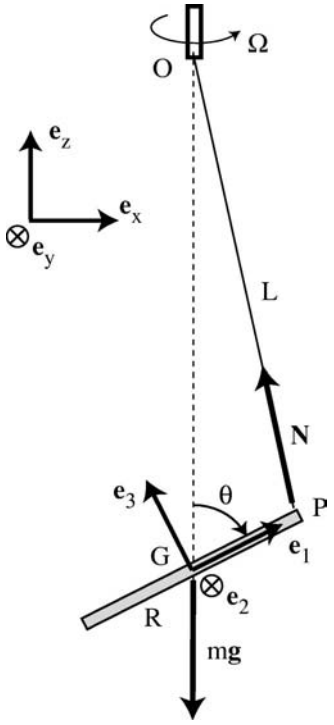

Fig. 1. A hoop of center of mass G, attached to a string OP, spins about the vertical axis OG, making angle θ to the vertical.

The equation of motion is derived from the Lagrangian function $\mathcal{L}=T-V$, where T is the kinetic energy and V is the potential energy.

The potential energy is $V=mgz_G$, where z_G is the center of mass elevation. In the limit of a long string, to first order in R/L, we just have $z_G=-R\cos\theta$, where the reference for V is taken at the horizontal hoop ($\theta=\pi/2$).

The kinetic energy T has two contributions: one from the translation of the center of mass, $T_{\rm tr}$, and one from the hoop rotation, $T_{\rm rot}$. The translational kinetic energy is simply $T_{\rm tr}=\frac{1}{2}m\dot{z}_G^2$. Using the same approximation for z_G as above, we can write $T_{\rm tr}=\frac{1}{2}mR^2\dot{\theta}^2\sin^2\theta$. The rotational kinetic energy is $T_{\rm rot}=\frac{1}{2}\boldsymbol{\omega}\cdot\tilde{I}\cdot\boldsymbol{\omega}$, where $\tilde{I}$ is the inertia matrix of the hoop relative to G. In the reference frame of the hoop, the inertia matrix $\tilde{I}$ has diagonal components $I_1=I_2=\frac{1}{2}mR^2$ and $I_3=mR^2$. Hence, with the total angular velocity (1), we have $T_{\rm rot}=\frac{1}{4}mR^2[\dot{\theta}^2+\Omega^2(1+\sin^2\theta)]$.

The Lagrangian function $\mathcal{L}=T_{\rm rot}+T_{\rm tr}-V$ can finally be written

$$\mathcal{L}=\tfrac{1}{4}mR^2[\dot{\theta}^2(1+2\sin^2\theta)+\Omega^2(1+\sin^2\theta)]+mgR\cos\theta. \tag{2}$$

Writing Lagrange's equation for the coordinate θ, we end up with the differential equation of motion

$$\ddot{\theta}(1+2\sin^2\theta)-(\Omega^2-2\dot{\theta}^2)\sin\theta\cos\theta+\Omega_c^2\sin\theta=0, \tag{3}$$

where we have introduced the critical angular velocity $\Omega_c=\sqrt{2g/R}$.

This equation of motion can also be obtained from the angular momentum equation and Newton's law. In the rotating frame of reference, the angular momentum equation reads

$$\frac{d\mathbf{L}}{dt}+\boldsymbol{\omega}\times\mathbf{L}=\boldsymbol{\Gamma}, \tag{4}$$

where $\mathbf{L}=\tilde{I}\boldsymbol{\omega}$ is the angular momentum and $\boldsymbol{\Gamma}=\mathbf{GP}\times\mathbf{N}$ is the torque due to the string tension, N, relative to the center of mass (the gravitational torque vanishes). The string tension is obtained from Newton's law,

$$m\ddot{z}_G\,\mathbf{e}_z=\mathbf{N}+m\mathbf{g}. \tag{5}$$

To first order in R/L, $\mathbf{N}$ is vertical, so its torque is simply $\boldsymbol{\Gamma}=-RN\sin\theta\,\mathbf{e}_2$. Using $z_G=-R\cos\theta$, we obtain

$$\boldsymbol{\Gamma}=-R(mg+mR(\dot{\theta}^2\cos\theta+\ddot{\theta}\sin\theta))\sin\theta\,\mathbf{e}_2. \tag{6}$$

Substituting (6) into Eq. (4) and considering only the $\mathbf{e}_2$ component, we finally recover the equation of motion (3).

B. Steady states and small oscillations

We are interested in the steady states for the pitch angle θ and the natural frequency for small oscillations about them. The steady states are obtained by letting $\dot{\theta}=\ddot{\theta}=0$ in Eq. (3). Two equilibrium solutions are found: in addition to the trivial solution $\theta_{\rm eq}=0$ for all Ω, a nontrivial solution exists for Ω above the critical value Ω_c,

$$\theta_{\rm eq}=\pm\cos^{-1}\left(\frac{\Omega_c}{\Omega}\right)^2, \tag{7}$$

which is plotted in Fig. 2(a). As expected, we have $\theta_{\rm eq}=0$ for $\Omega=\Omega_c$ (vertical hoop), and $|\theta_{\rm eq}|\to\pi/2$ in the limit of high rotation rate $\Omega\gg\Omega_c$ (horizontal hoop).

It is interesting to note that these steady states coincide with the ones from the bead-on-a-hoop problem,[4] whose equation of motion is

$$\ddot{\theta}-\Omega^2\sin\theta\cos\theta+\Omega_c^2\sin\theta=0. \tag{8}$$

The difference between Eqs. (3) and (8) originates from the translational kinetic energy of the center of mass, which has no counterpart in the bead-on-a-hoop problem. We can anticipate from (3) that this additional term will act as an increased effective inertia for nonzero angle θ of the spinning hoop.

It is often convenient to define the equilibrium positions as the minima of an effective potential $U(\theta)$ such that $\ddot{\theta}=-\partial U/\partial\theta$. This procedure can be readily applied from Eq. (8) for the bead-on-a-hoop, but clearly fails for the spinning hoop, because of the presence of the $\dot{\theta}$ term in Eq. (3). In other words, the effective force acting on the coordinate θ does not depend only on θ, but also on its derivative $\dot{\theta}$, i.e., the force is not conservative.

The stability and natural frequency for small oscillations are obtained by introducing in Eq. (3) a small perturbation in the form

$$\theta(t)=\theta_{\rm eq}+\delta\theta\,e^{(\sigma+i\omega)t}, \tag{9}$$

where $\theta_{\rm eq}$ stands for the trivial or nontrivial solution and $\delta\theta\ll1$. Since the problem involves no damping, the growth rate σ is zero when $\theta_{\rm eq}$ is stable (with a nonzero natural

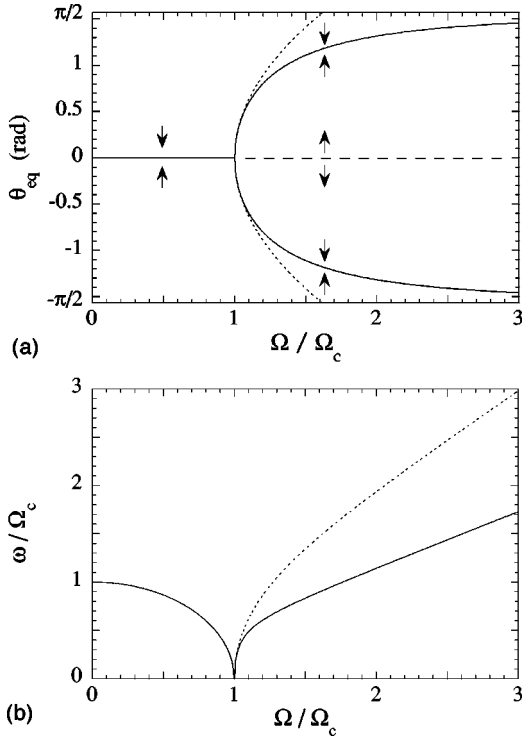

Fig. 2. (a) Equilibrium positions θ_{eq} as a function of the normalized angular velocity Ω/Ω_c. The arrows indicate the stability of the branches. The trivial branch $\theta_{eq}=0$ is stable for $\Omega<\Omega_c$ (———) and unstable for $\Omega\geqslant\Omega_c$ (– – – – –). The branch $\theta_{eq}\neq 0$ (7) is stable for $\Omega\geqslant\Omega_c$ (———). The small angle approximation (11) is also shown for $\Omega\geqslant\Omega_c$ (---------). (b) Natural frequency ω for small oscillations for the spinning hoop (———) compared to that of the bead-on-a-hoop (---------). For $\Omega<\Omega_c$, the two curves coincide. For $\Omega\gg\Omega_c$, we have $\omega\to\Omega$ for the bead-on-a-hoop, and $\omega\to\Omega/\sqrt{3}$ for the spinning hoop.

frequency ω) and positive when θ_{eq} is unstable.

The trivial solution $\theta_{eq}=0$ is found to be stable for $\Omega<\Omega_c$, with a natural frequency $\omega=(\Omega_c^2-\Omega^2)^{1/2}$, and unstable for $\Omega\geqslant\Omega_c$, with a growth rate $\sigma=(\Omega^2-\Omega_c^2)^{1/2}$ (and $\omega=0$). This is also valid for the bead-on-a-hoop, since the linearizations of Eqs. (3) and (8) about $\theta\simeq 0$ coincide. Above the transition, the nontrivial solution $\theta_{eq}\neq 0$ is always stable, with a natural frequency

$$\omega=\Omega\left[\frac{1-(\Omega_c/\Omega)^4}{3-2(\Omega_c/\Omega)^4}\right]^{1/2}. \tag{10}$$

In the case of the bead-on-a-hoop, the natural frequency,[4] $\omega=\Omega[1-(\Omega_c/\Omega)^4]^{1/2}$, takes larger values, as shown in Fig. 2(b). This difference comes from the above-mentioned additional inertia term in Eq. (3) for $\theta_{eq}\neq 0$, which tends to slow down the oscillations of the spinning hoop.

It is instructive to focus on the behavior of the solutions in the close vicinity of the bifurcation, $\Omega\simeq\Omega_c$. In terms of the reduced angular velocity $\epsilon=\Omega/\Omega_c-1$, the solutions become (for $|\epsilon|\ll 1$ and $\theta_{eq}\simeq 0$):

$$\begin{cases}\theta_{eq}=0 & \text{for } \epsilon<0,\\ \theta_{eq}\simeq 2\sqrt{\epsilon} & \text{for } \epsilon\geqslant 0,\end{cases} \tag{11}$$

which is the classical form of a supercritical pitchfork bifurcation.[3] Following the usual terminology, the pitch angle θ_{eq} is the order parameter and ϵ is the control parameter. For both solutions, one can see that the period of the oscillations and the growth time,

$$\omega^{-1}\sim\sigma^{-1}\propto|\epsilon|^{-1/2}, \tag{12}$$

diverge as one approaches the transition from both sides. This critical slowing down is the usual signature of supercritical bifurcation. However, it is worth noting that the small angle approximation (11) holds only very close to the bifurcation, as shown in Fig. 2(a), and the discrepancy between Eqs. (7) and (11) quickly becomes important as the control parameter in increased.

C. Nonlinear oscillations

When the oscillation amplitudes about the steady states are not small, the nonlinear terms in Eq. (3) become important and may affect the dynamics of the system. The orbits in the phase space $(\theta,\dot\theta)$ then provide a useful tool to characterize the nonlinear dynamics of the spinning hoop, and to compare it with the one of the bead-on-a-hoop (8). The equation of motion can be integrated using the Jacobi invariant,[8]

$$C=\dot\theta\frac{\partial\mathcal{L}}{\partial\dot\theta}-\mathcal{L}, \tag{13}$$

which takes a constant value along an orbit. This integral of the motion would simply correspond to the total energy in the case of a conservative system. However, there is no physical interpretation for this invariant here, because the system is not conservative.

The orbits in the phase space are obtained by numerically solving (using Mathematica) $C(\theta,\dot\theta)=\text{cst}$ for different values of the constant. Figure 3 shows such phase portraits for two forcing frequencies, below [$\Omega/\Omega_c=0.8$, Fig. 3(a)] and above [$\Omega/\Omega_c=1.2$, Fig. 3(b)] the transition, together with the orbits of the bead-on-a-hoop (dashed lines). One can clearly see the trivial solution $\theta_{eq}=0$ for $\Omega/\Omega_c=0.8$ and the two nontrivial solutions (7) separated by a saddle point at $\theta=0$ for $\Omega/\Omega_c=1.2$. Note that we are only interested in the closed orbits in the domain $|\theta|\leqslant\pi/2$: orbits that cross $\theta=\pm\pi/2$ are not consistent with the assumption that the point P remains the highest point of the hoop.

Around the stable fixed points, both systems show nearly elliptic orbits, as expected from small harmonic oscillations. Larger oscillations of the hoop show orbits with sharper corners around $\theta\simeq 0$, associated with larger angular velocities $|\dot\theta|$. This discrepancy originates from the vertical translation of the center of mass, which is responsible for an additional pitch angle acceleration when the hoop is nearly vertical.

D. Timescales

Two timescales are relevant for a practical experiment: the startup timescale of rotation τ_s and the damping timescale of oscillations τ_d. The startup timescale may be obtained considering the string torsion. We start from an initially vertical hoop ($\theta=0$), and then let its rotation angle ϕ about $\mathbf{e}_z$ be free. The string transfers a torque $\kappa(\phi-\Omega t)=\kappa\,\delta\phi$ to the hoop, where κ is the torsion constant and $\delta\phi$ is the string torsion. The angular momentum equation about $\mathbf{e}_z$ applied to the hoop then reads

$$\tfrac{1}{2}mR^2\delta\ddot\phi+\kappa\,\delta\phi=0. \tag{14}$$

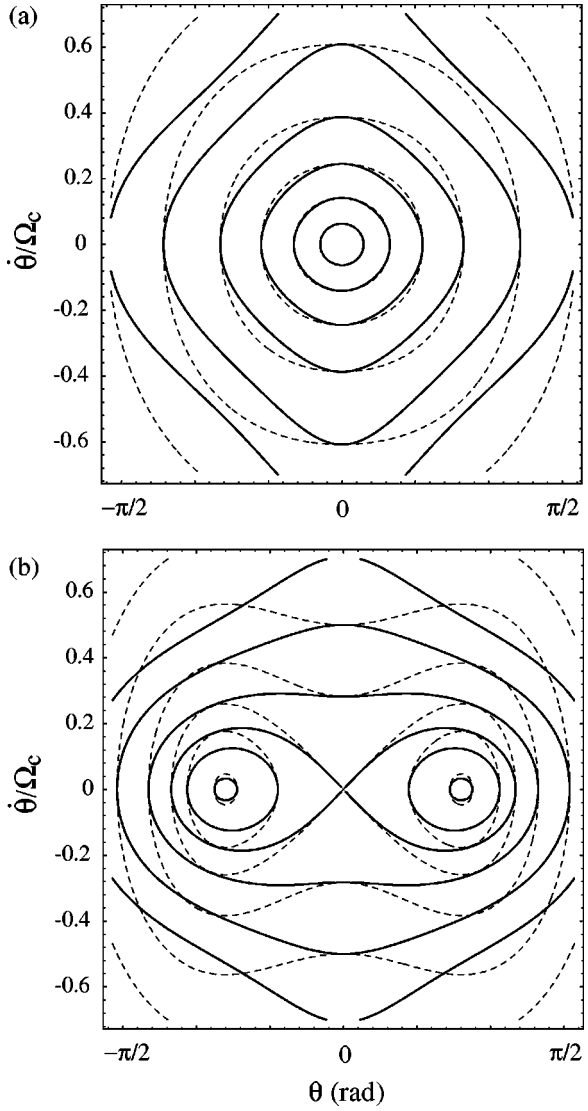

Fig. 3. Orbits in the phase space $(\theta, \dot{\theta}/\Omega_c)$ for the hula hoop (solid lines) compared to the bead-on-a-hoop (dashed lines). (a) $\Omega = 0.8\Omega_c$. (b) $\Omega = 1.2\Omega_c$.

Taking $\delta\ddot{\phi} \simeq \delta\phi/\tau_s^2$ gives the startup timescale $\tau_s \simeq R(m/2\kappa)^{1/2}$—which also corresponds to the period of the string torsion oscillations if no damping were present.

The damping timescale τ_d is relevant both for the ϕ oscillations due to the string torsion, and for the θ oscillations around the equilibrium states. It can be obtained considering the friction with the surrounding air. With a typical velocity of order m/s and hoop thickness w of a few millimeters, the air flow around the hoop is expected to be turbulent,[9] and the drag force on the hoop varies then as the square of the velocity. Neglecting $\dot{\theta}$ compared to $\dot{\phi}$, a unit length dl of the hoop experiences a drag force $df \simeq \rho(R\dot{\phi})^2 w\, dl$, where ρ is the air density. Integrating over the hoop perimeter leads to the frictional torque

$$\mathbf{\Gamma}_r \simeq -\rho R^4 \dot{\phi}^2 w \frac{\mathbf{\Omega}}{|\mathbf{\Omega}|}. \tag{15}$$

Hence the angular momentum equation about $\mathbf{e}_z$ reads

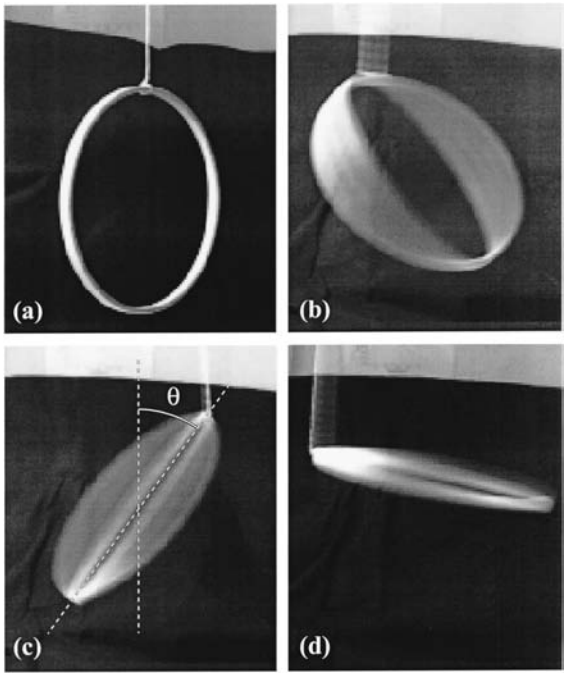

Fig. 4. Pictures of the hoop. (a) The hoop at rest. (b) and (c) $\theta \simeq 37°$. (d) $\theta \simeq 78°$. In picture (c) the procedure used to measure the angle θ is shown.

$$\ddot{\phi} + \left(\frac{\rho_0}{\rho}\frac{w}{R}\right)\dot{\phi}^2 = 0, \tag{16}$$

where ρ_0 is the hoop density. Taking $\dot{\phi} \simeq \Omega$ and $\ddot{\phi} \simeq \Omega/\tau_d$, the damping timescale finally becomes

$$\tau_d \simeq \left(\frac{\rho_0}{\rho}\frac{w}{R}\right)\Omega^{-1}. \tag{17}$$

For values of practical interest, τ_d is of order of a few tens of the rotation period Ω^{-1}. Note here that in the case of the hula hoop game, the rolling friction on the player's hips is fortunately dominant, leading to a damping timescale of order Ω^{-1}.

III. EXPERIMENTAL RESULTS

An experiment has been carried out using a wooden hoop ($\rho_0 \simeq 0.67$ g.cm^{-3}) of mass $m = 15.5$ g, radius $R = 86$ mm, and cross-sectional area 4×10 mm^2. The expected frequency threshold is then $\Omega_c/2\pi \simeq 2.40$ Hz (classical hula hoops have $\Omega_c/2\pi \simeq 1$ Hz). A simple cotton thread, of length $L = 0.68$ m and mass less than 3% of the hoop mass, was fixed to a constant current motor. The startup timescale for this string can be estimated from the free oscillation period, $\tau_s \simeq 5$ s (corresponding to a torsion constant $\kappa \simeq 2 \times 10^{-6}$ N.m). This string is far from being rigid, and during the early stage of the rotation, torsional energy is stored in the string. The string progressively transfers rotation to the hoop, and the fluctuations (due to a varying imposed rotation rate at its upper end, or to pitch angle variation at the other end) are smoothed down on a timescale τ_d.

Figure 4 shows pictures of the spinning hoop for different angular velocities Ω, obtained from a simple CCD camera. Seen from the side, the hoop appears as an ellipse. The pictures are somewhat blurry, because the time aperture of the

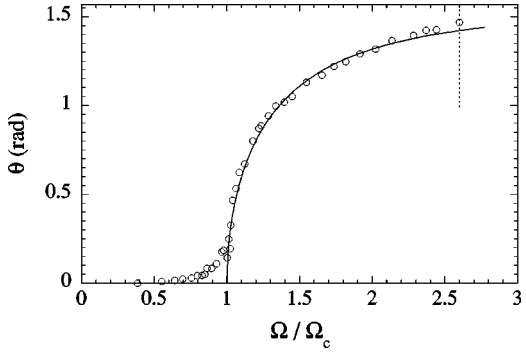

Fig. 5. Bifurcation diagram of the pitch angle θ as a function of the normalized angular velocity Ω/Ω_c. The solid line is the calculated solution Eq. (7), with Ω_c adjusted to fit the experimental data.

camera, $\simeq$40 ms (25 frames per second), is not negligible compared to the rotation timescale, $(\Omega_c/2\pi)^{-1}\simeq 400$ ms. On frames where the ellipse is nearly in profile, as in Figs. 4(c) and 4(d), the pitch angle θ can be easily measured to within 1°.

The measured pitch angles θ, shown in Fig. 5, are in excellent agreement with the exact solution Eq. (7), except for low rotation rate, where nonzero angles are measured below the expected transition. The experimental frequency threshold, obtained by extrapolating the curve down to $\theta\simeq 0$, is $\Omega_c/2\pi\simeq(2.30\pm 0.03)$ Hz, which agrees within 5% with the theoretical value. The discrepancy at low rotation rate is typical of an imperfect bifurcation, where a small asymmetry in the apparatus (such as the position of the knot) slightly anticipates the destabilization of the basic state.

An interesting observation is that, for $\Omega\geqslant 2.6\Omega_c$ (see the dashed line in Fig. 5), the bifurcated state is not stable any more: a secondary instability appears, in the form of a slow precession of the center of mass, with a period of about ten rotation periods. This new behavior is probably an effect of the nonzero mass of the string, and clearly can not be described in our calculation, where the hoop center of mass is constrained to remain on the vertical axis.

Transient phenomena may also be investigated by means of the usual video processing. An illustration is given in Fig. 6, showing a spatio-temporal diagram obtained by collecting the light intensity recorded on a horizontal line passing through the string. In this example, the imposed frequency $\Omega/2\pi$ has been suddenly increased from 0 to 5.5 Hz $\simeq 2.4\ \Omega_c/2\pi$ (first arrow). One can see that, after a transient time of around 7 s (second arrow) during which the string rotation propagates down to the hoop, the amplitude increases and saturates to a finite value.

From this diagram, the instantaneous pitch angle as well as the instantaneous oscillation frequency $\dot{\phi}/2\pi$ may be extracted, as shown in Fig. 7. The frequency is obtained from averaging over six successive oscillations. Due to the progressive torsion of the string, this frequency slowly approaches its imposed value 5.5 Hz. As a consequence, the increase of the pitch angle towards its stationary value $\theta_{\rm eq}$ $\simeq 1.40$ rad is rather slow.

It is interesting to note that, when plotting the instantaneous pitch angle as a function of the instantaneous frequency (see Fig. 8), the bifurcation diagram of Fig. 5 is recovered to a high degree of accuracy. This suggests that the pitch angle follows ''adiabatically'' the instantaneous frequency so that the apparent growth rate is essentially controlled by the string torsion more than by the intrinsic dynamics of the instability (at least far from the transition).

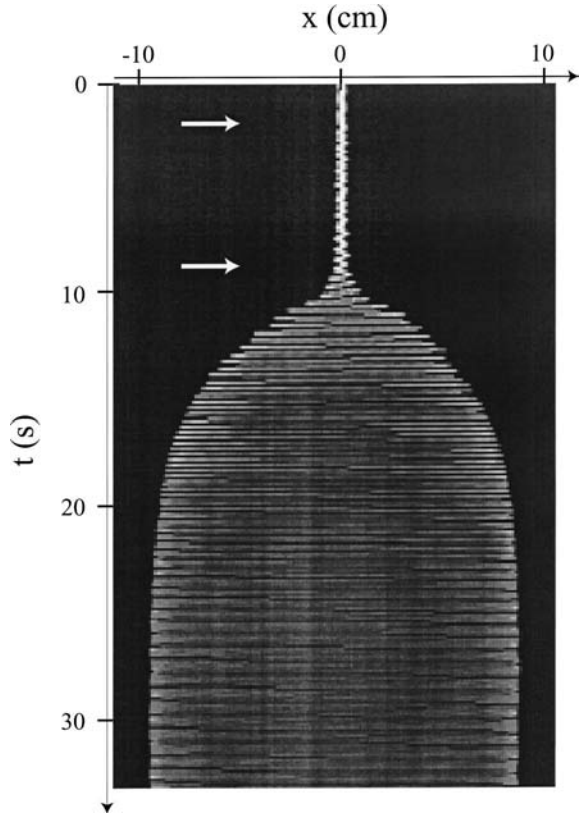

Fig. 6. Spatio-temporal diagram of the light intensity recorded on a horizontal line, showing the string oscillation, when the frequency $\Omega/2\pi$ is increased from 0 to 5.5 Hz.

IV. DISCUSSION

This simple experiment provides an interesting alternative to the bead-on-a-hoop[4–7] experiment as a mechanical analog to bifurcation and second-order phase transition in physics. Close attention does not need to be paid to the choice of the material and the experimental conditions, making this experiment one that is easy to perform by undergraduate students. Further experiments can be carried out, e.g., studying

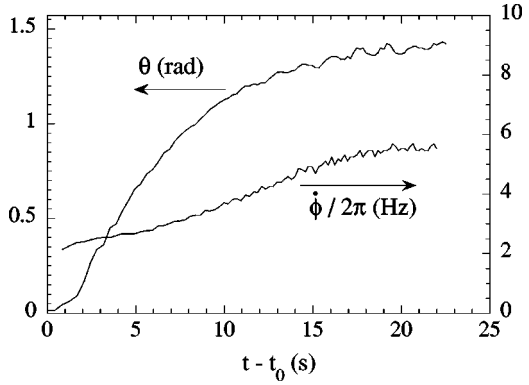

Fig. 7. Instantaneous pitch angle θ (left) and rotation frequency $\dot{\phi}/2\pi$ (right) as measured from Fig. 6. The origin time t_0 corresponds to the second arrow in that figure.

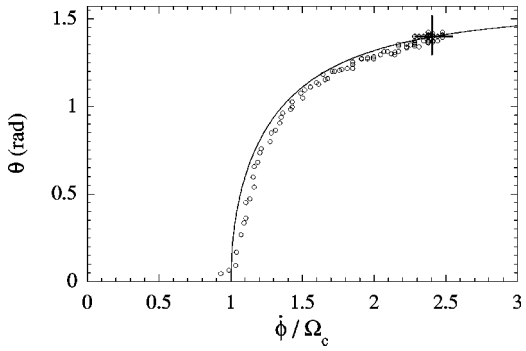

Fig. 8. Instantaneous pitch angle θ as a function of the instantaneous rotation frequency $\dot{\phi}/\Omega_c$ (same data as in Fig. 7). The solid line is the calculated solution (7), as in Fig. 5. The cross indicates the stationary solution $\theta_{\mathrm{eq}} \simeq 1.40$ rad for $\Omega = 2.4\ \Omega_c$.

the transient phenomena resulting from a small perturbation. As a suggestion, one may restrain the point P on the vertical axis when $\Omega > \Omega_c$ by means of a small hook around the string. Releasing the hook lets us measure the growth rate and characterize its divergence as $\epsilon \to 0$. This method can be hardly achieved with a bead-on-a-hoop apparatus as access is inherently difficult.

Another motion may compete with the bifurcation described in this paper: the hoop can rotate as a whole about the vertical axis, its center of mass remaining aligned with the string. This is the usual motion for the conical pendulum, which also leads to a supercritical bifurcation with a threshold simply given by the natural frequency $\omega_0 \simeq \sqrt{g/(L+R)}$. The conical pendulum motion overcomes the spinning hoop motion for ω_0 of order of Ω_c, i.e., for a string length of order of the hoop radius. Moving the center of mass away from the vertical axis may allow us to observe the competition between the two regimes, even for a longer string.

Similar bifurcations as the result of a competition between centrifugal force and gravity are present in a number of situations. Spinning plates provide an interesting illustration just as for the hula hoop, except that the motion is forced by the precession of the rigid rod rather than its rotation. The imposed precession frequency has to overcome the natural frequency for the plate to stand up, and then the horizontal state is maintained by a parametric oscillation mechanism.[10] Lasso roping is another example, where the rigid hoop is replaced by a deformable loop. Here again the motion is maintained by the precession of the rope rather than rotation. As a consequence, the knot on the loop makes the rope rotate as well, so that it has to be continuously untwisted at its other end.

Note that this experiment can be carried out with any rigid body, not necessarily axisymmetric. In this case, the angle of the equilibrium state (7) remains unchanged, and the angular velocity threshold just becomes $\Omega_c = \sqrt{mga/(I_3 - I_1)}$, where $a = |\mathbf{GP}|$ is the distance between the center of mass and the knot. Note, however, that for bodies with three different moments of inertia, in addition to the bifurcation described here, inertial instabilities may also occur. Such an instability involves the roll angle about $\mathbf{e}_1$ as an additional degree of freedom, and is not described by our calculation.

ACKNOWLEDGMENTS

This work has benefited from fruitful discussions with Olivier Martin, Bernard Perrin, and Marc Rabaud. Thanks to Inigo Fraser Jenkins for his careful reading of the manuscript.

[a]Electronic mail: moisy@fast.u-psud.fr

[1]Donald T. Greenwood, *Principles of Dynamics*, 2nd ed. (Prentice-Hall, Englewood Cliffs, NJ, 1988), Sec. 8-1.
[2]H. Keith Moffatt, "Spinning eggs—a paradox resolved," Nature (London) **416**, 385–386 (2002).
[3]Philip G. Drazin, *Nonlinear Systems* (Cambridge U.P., Cambridge, 1992), pp. 1–48.
[4]Jean Sivardière, "A simple mechanical model exhibiting a spontaneous symmetry breaking," Am. J. Phys. **51** (11), 1016–1018 (1983).
[5]Glenn Fletcher, "A mechanical analog of first- and second-order phase transitions," Am. J. Phys. **65** (1), 74–81 (1997).
[6]Richard V. Mancuso, "A working mechanical model for first- and second-order phase transitions and the cusp catastrophe," Am. J. Phys. **68** (3), 271–277 (2000).
[7]N. Sungar, J. P. Sharpe, M. J. Moelter, N. Fleishon, K. Morrison, J. McDill, and R. Schoonover, "A laboratory-based nonlinear dynamics course for science and engineering students," Am. J. Phys. **69** (5), 591–597 (2001).
[8]See Ref. 1, Sec. 6-8.
[9]Etienne Guyon, Jean-Pierre Hulin, Luc Petit, and Catalin D. Mitescu, *Physical Hydrodynamics* (Oxford U.P., Oxford, 2001), Sec. 11.
[10]Thomas K. Caughey, "Hula-Hoop: An Example of Heteroparametric Excitation," Am. J. Phys. **28**, 104–109 (1960).